Diagn Interv Radiol 2024; DOI: 10.4274/dir.2024.242926

MODALITY-BASED (UC, CT, MRI, PET-CT) IMAGING

INVITED REVIEW

New imaging techniques and trends in radiology

Mecit Kantarcı[1]
Sonay Aydın[2]
Hayri Oğul[3]
Volkan Kızılgöz[2]

[1]Atatürk University Faculty of Medicine, Department of Radiology, Erzurum, Türkiye

[2]Erzincan Binali Yıldırım University Faculty of Medicine, Department of Radiology, Erzincan, Türkiye

[3]Medipol University Faculty of Medicine, Department of Radiology, İstanbul, Türkiye

ABSTRACT

Radiography is a field of medicine inherently intertwined with technology. The dependency on technology is very high for obtaining images in ultrasound (US), computed tomography (CT), and magnetic resonance imaging (MRI). Although the reduction in radiation dose is not applicable in US and MRI, advancements in technology have made it possible in CT, with ongoing studies aimed at further optimization. The resolution and diagnostic quality of images obtained through advancements in each modality are steadily improving. Additionally, technological progress has significantly shortened acquisition times for CT and MRI. The use of artificial intelligence (AI), which is becoming increasingly widespread worldwide, has also been incorporated into radiography. This technology can produce more accurate and reproducible results in US examinations. Machine learning offers great potential for improving image quality, creating more distinct and useful images, and even developing new US imaging modalities. Furthermore, AI technologies are increasingly prevalent in CT and MRI for image evaluation, image generation, and enhanced image quality.

KEYWORDS

Arthrographic applications, cerebrospinal fluid flowmetry, imaging techniques, magnetic resonance spectroscopy, magnetic resonance imaging techniques

Medical imaging is the process of generating visual representations of the body's tissues and organs to examine their structure and function for clinical and scientific purposes. These techniques allow the evaluation of internal structures beneath the skin and bones, facilitating the diagnosis of abnormalities and the treatment of diseases. Medical imaging has become an essential component of healthcare, research, and biological imaging.[1,2]

Imaging technologies play a critical role in diagnosing abnormalities and supporting therapy, providing medical personnel with essential information about their patients' conditions. Techniques such as electroencephalography (EEG), magnetoencephalography (MEG), and electrocardiography capture and quantify data rather than generate visuals. They present information as parameter graphs over time or maps with varying levels of detail. Although these technologies have limitations, they can be considered a form of medical imaging on a smaller scale. By 2010, more than 5 billion medical imaging studies had been completed worldwide.[3]

Medical imaging accounts for approximately 50% of the overall ionizing radiation exposure in the United States. These technologies are crucial for the diagnosis, management, treatment, and prevention of various disorders. Imaging techniques are now essential for diagnosing nearly all major medical conditions, including trauma, malignancies, cardiovascular diseases, neurological disorders, and numerous other health issues. These techniques are operated by highly skilled technicians and medical specialists, such as oncologists and internists.[1]

Medical imaging technologies are predominantly used for medical diagnostics. Diagnosis refers to the systematic identification of a patient's condition and associated symptoms. The process involves gathering data from the patient's medical history, physical examinations, or

Corresponding author: Mecit Kantarcı

E-mail: akkanrad@hotmail.com

Received 28 September 2024; revision requested 18 November 2024; accepted 04 December 2024.

Epub: 16.01.2025

Publication date: xx.xx.2025

DOI: 10.4274/dir.2024.242926

You may cite this article as: Kantarcı M, Aydın S, Oğul H, Kızılgöz V. New imaging techniques and trends in radiology. *Diagn Interv Radiol*. 16 January 2025 DOI: 10.4274/dir.2024.242926

questionnaires to determine the appropriate course of treatment. However, diagnosis can be challenging, as many indications and symptoms are non-specific in nature. For example, the presence of erythema, which is characterized by redness of the skin, may indicate a variety of disorders. Therefore, distinct diagnostic methods are required to identify the etiology of diseases and determine appropriate treatment or preventive measures.[4,5]

Historically, ancient physicians made medical diagnoses based on visual and auditory observations, occasionally supplemented by the examination of human specimens. For example, techniques such as examining bodily fluids, including urine and saliva, were commonly practiced before 400 B.C. In ancient Egypt and Mesopotamia, physicians were capable of diagnosing conditions related to the gastrointestinal and cardiovascular systems, cardiac rhythm, spleen, liver, and menstrual disorders. However, medical interventions were primarily limited to affluent and noble individuals.[5]

Hippocrates, who lived around 300 B.C., advocated the use of the mind and senses as diagnostic tools, earning him the title of the "Father of Medicine." He promoted a diagnostic process that included urine testing, skin color observation, and the examination of the lungs and other external indicators. He also observed the correlation between illness and heredity. Abu al-Qasim al-Zahrawi, an Arabic physician of the Islamic era, documented the first recorded instance of a hereditary genetic disorder, now known as hemophilia. He provided a detailed account of a family in Andalusia in which the males were affected by this condition.[5]

During the Middle Ages, physicians employed various methods to determine the origins of physical imbalances. Uroscopy, the predominant technique, involved collecting the patient's urine in a specialized container called a "matula" and analyzing its color, odor, density, and the presence of precipitates. Physicians also examined the consistency and color of blood to distinguish between chronic and acute conditions. Pulse rate, strength, and rhythm were evaluated through palpation. Additionally, medical practices during this period often incorporated the interpretation of zodiac signs.[6]

In the 19th century, the introduction of diagnostic equipment such as X-rays and microscopes brought about a significant transformation in the field of diagnosing and treating disorders. In the early part of the century, doctors predominantly diagnosed diseases by analyzing symptoms and indications. During the 1850s, the use of instruments such as ophthalmoscopes, stethoscopes, and laryngoscopes enhanced doctors' sensory capabilities, leading to the development of novel diagnostic methods and approaches. During this era, a variety of diagnostic techniques were developed, including chemical testing, bacteriological tests, microscopic examinations, X-rays, and several other medical tests.[5,6]

The development of X-rays marked substantial advancements in medical imaging procedures. Wilhelm Conrad Roentgen discovered X-rays in November 1895, a discovery that earned him the Nobel Prize in 1901. Initially, radiologists used the term "plane film" to describe X-rays, employing them to diagnose bone fractures and chest abnormalities. Fluoroscopy, with its enhanced X-ray beam, facilitated the detection of a wide range of patient issues. In the 1920s, radiologists began using these procedures to diagnose disorders such as esophageal cancer, ulcers, and stomach conditions. Fluoroscopy ultimately evolved into computed tomography (CT).[7]

Numerous advanced imaging techniques have been developed, each with its principles, applications in medical labs, and advancements over time. The following techniques are essential for understanding their benefits and uses in diagnosing, managing, and treating various diseases, including cardiovascular conditions, cancer, neurological disorders, and trauma.

Main points

- Computed tomography (CT) scans will continue to be an essential part of contemporary medical diagnostics thanks to developments in resolution, velocity, radiation dose reduction, artificial intelligence (AI) integration, and personalized treatment. The development of portable CT scanners and the use of functional and multimodal imaging will enhance this technology's potential.
- Advancements in magnetic resonance imaging (MRI) systems are meant to improve accessibility, shorten scan times, and produce better-quality images in areas where MRI has historically had difficulties.
- AI technology can produce results from ultrasound (US) exams that are more accurate and consistent. The application of machine learning to US imaging has great potential to improve image quality, produce more unique and useful images, and possibly introduce new US imaging methods.
- Across all modalities, AI technologies are increasingly being used and showing an increased trajectory in both image production and evaluation.

Advancements across modalities

1. Computed tomography

CT uses X-rays to generate highly detailed cross-sectional images of the body. The high-resolution imaging of tissues and organs aids in diagnosing internal injuries, cancers, and other illnesses. Hounsfield developed the first iteration of a CT scanner in the 1960s. CT, commonly known as X-ray CT, was first implemented in 1971 at Atkinson Morley Hospital in Wimbledon (now part of St George's Hospital). Sir Godfrey Hounsfield performed this pioneering brain scan under the guidance of Jamie Ambrose, MD, an expert neuroradiologist. The objective of the scan was to investigate less painful alternatives to existing methods of brain examination. CT technology has undergone significant developments since its introduction in the 1970s. These advancements have revolutionized the field of diagnosis and treatment planning by using X-rays and advanced algorithms to produce highly detailed cross-sectional images. The scanner designs used for image formation in CT are called generations. New generations have emerged with different arrangements of components and mechanical movements required for data collection. The main differences between CT generations relate to the number and arrangement of detectors, the shape of the X-ray beam, and the rotation of the tube and detectors. Based on a recent analysis by Mordor Intelligence, the CT market is projected to experience significant growth, with its value expected to rise from $8.14 billion in 2023 to $10.95 billion by 2028. This growth is anticipated to occur at a compound annual growth rate of 6.12%.[8]

The introduction of dual-energy CT (DECT) technology marked a substantial departure from traditional methods and paved the way for contemporary advancements in CT technology. DECT is a well-established technology with a significant and extensive background. Sir Godfrey Hounsfield devised a technique in the 1970s to differentiate calcium from iodine by using two distinct energy spectra from X-ray photons. This method relies on understanding the specific atomic numbers and unique K-edge characteristics of various substances. These features are essential for discerning the differing impacts of Compton scattering and the photoelectric effect in X-ray attenuation.[9]

In the early 1980s, DECT technology was primarily used for bone densitometry, as demonstrated by devices such as the Somatom DR manufactured by Siemens Healthcare. This device employed rapid tube potential switching to acquire two-photon energy spectra. Because of the limited computing capabilities of the hardware available at the time, DECT was mainly used for densitometry purposes. However, the 21st century witnessed notable progress in the therapeutic use of DECT, driven by rapid advancements in processing capabilities. During this period, scanners with dual sources, such as the Somatom Definition DS in 2006 and the Somatom Definition Flash in 2009, were introduced. Additionally, multilayer detectors, such as the Brilliance-64 in 2015, were also introduced. In 2010, General Electric Healthcare improved the technique of rapid tube potential switching with models such as the Revolution GSI and Discovery 750 HD.[10]

DECT enables the capture and reconstruction of a wide range of images. The kilovolt peak (kVp) images generated by DECT closely resemble those obtained from single-energy CT, as they replicate the characteristics of a single-energy spectrum. These images can be acquired using dual-layer, rapid kVp-switching, and split-filter DECT techniques. Dual-source DECT generates images by using a pair of kVp values or kVp-equivalent images, which are calculated by combining data from two distinct peaks using a weighted average. As a result, the reconstructions resemble images obtained using a single, user-selected kVp value. Virtual monoenergetic imaging replicates scans using photons at a specific energy level, which is advantageous due to the increased iodine attenuation at lower photon energy levels. In addition, material decomposition techniques exploit the different effects of Compton scattering and the photoelectric effect on X-ray attenuation. This allows for the production of images with enhanced or reduced iodine visibility and the exclusion of urine or calcium.[9,11]

Current studies on the cost-effectiveness of DECT reveal partially conflicting results for different areas of use. Although its use for incidental renal lesions and in the emergency department reduce costs, it is noted that the costs of cardiovascular system imaging sometimes increase. From this perspective, detailed studies on more specific usage areas are needed to determine the cost-effectiveness of DECT.[12-14]

Table 1 provides a summary of the areas in which DECT is used substantially more frequently. Recent studies suggest that it may also be beneficial in the evaluation of pulmonary perfusion, myocarditis, and the diagnosis of alveolar echinococcosis. These applications are in addition to those mentioned above.[15-18]

After August 2022, the Food and Drug Administration (FDA) approved two biomedical imaging technologies, developed in collaboration with the National Institute of Biomedical Imaging and Bioengineering (NIBIB), to be used in clinical settings. Both methods offer improvements in CT. Dr. Cynthia McCollough, the project lead and director of Mayo Clinic's CT Clinical Innovation Center, and her team have made a significant advancement by developing the first photon-counting detector (PCD)-CT system. This new system outperforms current CT technology and was described as the first major imaging advancement cleared by the FDA for CT in a decade.

Photon-counting CT (PCCT) is an advanced technological development in the field of energy-resolving, direct-conversion X-ray detectors. After 15 years of thorough study and development, this technique has recently been integrated into clinical CT equipment. The fundamental concepts of PCCT differ greatly from those of traditional CT detectors. The detectors used in traditional CT are known as energy-integrating detectors. These provide signals that are directly proportional to the total energy of photons received within a specific measurement interval. PCCT, however, uses PCDs to directly convert the energy of individual photons into electrical impulses. The device exclusively emits electrical pulses with heights exceeding the thresholds indicative of noise.[5] Therefore, this technology enables a significant reduction in electrical noise levels and an increase in the signal-to-noise ratio (SNR). Furthermore, it can also be utilized in dual-energy imaging. The advent of PCCT has the potential to transform the clinical CT field by leveraging its multiple inherent advantages and overcoming several constraints present in existing cutting-edge CT systems (Figure 1).[9] DECT requires specialized equipment and is limited to two energy levels. However, with the introduction of this novel detector, additional "buckets" are available to categorize X-ray energies, enhancing the ability to accurately represent material differences.

Table 1. DECT applications

Region	Material categorization/virtual monoenergetic beam	Quantification of iodone
Brain	Used to differentiate between tumors and bleeding	Used to distinguish between bleeding and contrast
Cardiac	Using low virtual monoenergetic KeV contributes to imaging myocardial fibrosis	
Lung		COVID-19 shows high iodine density around pulmonary opacity and increased perfusion in the lung parenchyma Reduced perfusion in the lung parenchyma within the area of pulmonary infarct indicates possible hypoperfused lung or pulmonary embolism.
Abdomen	Differentiates a hypoperfused segment of the bowel wall from one that is normally perfused Distinguishes between different types of tumors Aids in analyzing the composition of distinct kidney or gallstones	Iodine map imaging helps to better visualize iodine accumulation in the bowel wall, thereby improving diagnostic certainty for intramural hemorrhage
Vasculer imaging	Reduces the impact of blooming artifacts from calcified plaques	
Bones	VNC images can be used to distinguish chronic fractures from acute and non-displaced CT occult fractures	
Metallic artifacts	A high monoenergetic beam can help minimize metallic artifacts	

DECT, dual-energy computed tomography; COVIF-19, coronavirus disease-2019; VNC, virtual non-contrast images; CT, computed tomography.

Published in the Journal Radiology, clinical investigations have demonstrated that the new PCCT devices can effectively reduce noise by up to 47%. In addition, the new technique reduces the amount of contrast agent required for CT imaging. Due to the enhanced signal provided by the PCCT system, participants in the trial were able to achieve the same image quality as conventional CT systems using 30% less contrast agent. The PCCT systems offer superior spatial resolution compared with conventional systems, delivering the highest reported resolution for a clinical CT system.[19,20] Siemens developed a prototype PCD-CT system, and with financial support from McCollough through NIBIB, the team began scanning patients with approval from the Institutional Review Board. A total of 1,100 patients were examined in these tests, initially using a traditional CT system and subsequently with the advanced PCCT scanner, showcasing the benefits of the new technology. This device is the first product of its category available on the market.[20]

Another CT-based method approved by the FDA is artificial intelligence (AI)-assisted CT perfusion (CTP) imaging. An AI software was developed to assist in image reconstruction to reduce the elevated radiation dose in CTP. This software employs the K-space weighted image average technique to reduce noise in CTP images, resulting in lower radiation exposure for patients without compromising image processing quality or speed. Research has demonstrated that the software effectively decreases the radiation exposure of CTP by 50%–75% compared with the conventional CTP approach. Additional benefits of using this approach include no interruptions to the regular clinical workflow and no requirement for upgrades or modifications to existing CT hardware. The software has received FDA 510(k) clearance and is eligible for integration into clinical practice.[21]

The prospects for CT technology in the future are highly encouraging for both healthcare providers and patients. Advancements in resolution, velocity, radiation dose reduction, AI integration, and personalized medicine will ensure that CT scans remain a crucial component of modern medical diagnostics. The use of functional and multimodal imaging, along with the development of portable CT scanners, will further enhance the capabilities of this technology. In the future, the continuous progress of CT technology will lead to greater accuracy in diagnosis, improved treatment outcomes, and enhanced patient care.

Nowadays, thanks to advances in CT technology, especially cone beam and dual-source CT, arthrography is used in the diagnosis of many musculoskeletal pathologies. Compared with conventional magnetic resonance imaging (MRI) and MR arthrography, CT arthrography is superior in depicting chondral/osteochondral damage, loose bodies, chondral variations, and subarticular bone fractures.[22-27] Moreover, CT arthrography has excellent spatial resolution with multiplanar imaging capability and shorter examination times. Other indications for CT arthrography include patients with non-MRI-safe implantable devices or cardiac pacemakers and individuals with claustrophobia.[24,28]

Cone beam or flat-panel detector CT technology uses a cone-shaped X-ray beam and applies software programs with sophisticated algorithms, including back projection. Because of its perfect high spatial resolution, cone beam CT arthrography allows the optimal evaluation of cartilage and subchondral bone microarchitecture in the articular surface.[29,30] Recent studies have reported that cone beam CT scans can obtain images with very high resolution (75–300 µm slice thickness) with low-dose applications.[30-32] Lower radiation doses in cone beam CT technology are achieved through the smaller field of view, the use of a high-quality flat-panel detector system, and pulsed X-ray beams.[33]

In DECT, two different datasets are acquired at different voltage peak levels to separate materials based on tissue composition (e.g., urate mineralization, calcification, and iodine). This technique allows for the detection of gout tophi and the demonstration of bone marrow edema in vertebral compression fractures.[34,35] Recently, DECT has also been used to distinguish intra-articular iodinated contrast media from adjacent bone in CT arthrographic applications.[36-38]

2. Advancements in magnetic resonance imaging techniques and features

MRI was first implemented as a clinical diagnostic instrument in the early 1980s. Significant technological developments have occurred since its introduction. Advancements in various technical components, including data acquisition, image reconstruction, and hardware systems, have greatly impacted and propelled growth in other areas of MRI technology. The advancements in each component have generated new opportunities for growth in the others. Moreover, the swift integration of cutting-edge technologies derived from fundamental sciences and technical disciplines such as computer science, data processing, and semiconductors has resulted in revolutionary advancements in MRI technology (Figure 2).

Initial developments in MRI techniques focused on optimizing data acquisition protocols to achieve adequate spatial and temporal resolution, contrast, and imaging efficiency. An example of this delicate balance is the implementation of line reductions in the basic spin-echo protocol. However, this method has a drawback-the absence of frequency data, leading to a reduction in either image quality or image dimensions. Scanning time was reduced in methods such as the fast spin echo, echo planar imaging, or multi-echo approach by recording multiple lines following the radio frequency (RF) pulse. Despite the improvement, a major limitation was the rapid decline in signal intensity caused by energy transfer during T2 capture. This limitation allowed only 3–4 lines per RF pulse and led to a noticeable degradation in image quality.[39]

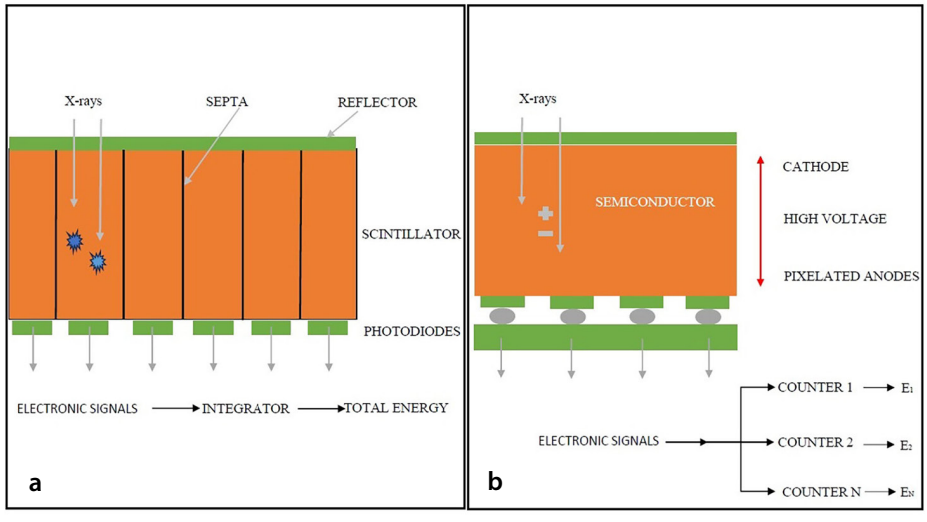

Figure 1. Illustrations of traditional CT (**a**) and photon-counting CT (**b**) detectors. CT, computed tomography.

2a. Acquisition procedures: advancements in parallel imaging techniques

Parallel imaging is currently employed in almost all clinical MRI scans to enable fast data capture for several reasons. Abdominal and cardiac scans often require patients to hold their breath to facilitate shorter scanning times. In certain situations, such as when multiple sequences occur after excitation pulses, blurring artifacts can arise, especially in imaging techniques such as turbo spin echo, due to significant T2 relaxation. These artifacts occur during the decomposition process while retrieving the lines. In other contexts, swift data collection is crucial to obtain extensive datasets efficiently.[40]

Parallel imaging reduces scanning time by using phased array coils to capture distinct perspectives of the tissue, thereby avoiding the need to scan a large portion of the region subjected to gradient encoding. However, the sensitivity of each coil element decreases rapidly with distance, which limits data collection to a specific tissue profile. A comprehensive image is generated by combining individual images from each coil. The maximum acceleration factor in parallel imaging is directly proportional to the number of coils. Typically, parallel imaging techniques employ coil arrays consisting of 4–8 coils. However, arrays with 32 or even 128 channels are available, particularly in cardiac imaging, resulting in a significant reduction in scanning time.

2b. Methods for reconstructing images for analysis

To prepare the data for meaningful information extraction, the initial steps of image capture, preprocessing, and segmentation are essential. During these processes, irrelevant or noise-based signals are eliminated. Patient movement is a common cause of noise. Sequential images are registered to correct motion artifacts, a process that can be achieved using algorithms specifically designed for medical imaging. The Insight ToolKit is currently considered the standard for MRI registration. It offers a range of algorithms for various operations, including transformations, similarity metrics, and contrast normalization.[41]

Machine learning applications have been increasingly used in recent trends in preprocessing and segmentation, such as denoising. Feature identification and classification have become important trends in machine learning techniques, primarily because these tasks require a large amount of manual effort. The abundance of imaging data obtained from MRI scans has increased the complexity of clinical diagnoses relying on MRIs, prompting the development of automated methods for data extraction and interpretation. Machine learning relies on algorithms generated from neural network architectures. These structures consist of nodes connected by weighted edges. Nodes receive inputs, multiply them by a set of parameters called weights, and then transport the resulting outputs through transfer functions such as sigmoid and hyperbolic tangent functions.[42]

Multi-information sourcing refers to the process of gathering and obtaining multiple sources of information. Models that use multiparametric techniques offer the substantial benefit of examining correlations between a large number of quantitative parameters, potentially leading to significantly improved accuracy. This contrasts with methods that analyze data using only one parameter. The time it takes for longitudinal (T1) and transverse (T2) relaxation, as well as the production of classical MR contrasts after the event, are all important metrics that can be obtained through MRI. However, this list is not exhaustive. Monitoring these metrics is done in conjunction with cutting-edge techniques for rapidly collecting data and performing computer analysis.[39]

Contemporary multiparametric analytical techniques use similar methods. These methods involve sampling both parameters and K-spaces simultaneously. These techniques require adjusting the collection parameters to capture data on the transient state, followed by undersampled K-space snapshots after each stimulation. Consequently, parametric maps are generated using a physical model based on the Bloch equations. Magnetic resonance fingerprinting (MRF) and quantitative transient-state imaging (QTI) are two examples of the various methods created as a direct outcome of this methodology.[43,44]

Modern multiparametric analytical techniques use similar methods by simultaneously sampling both parameters and K-spaces. These methods involve gathering transient-state data by adjusting the collection parameters and obtaining undersampled K-space snapshots after each stimulation. Parametric maps are generated using a physical model based on the Bloch equations. The methodologies of MRF and QTI have led to the development of these techniques.[45]

MRF is a technique that involves altering the settings of MRI sequences over time. This results in a series of MRI images with different weighting, and each type of tissue has a distinct MRI signal fingerprint. These fingerprints can be simulated using computational methods to generate a collection of tissue-specific fingerprints. During image reconstruction, the fingerprints obtained from the MRI data are compared with a dictionary. The fingerprint with the highest correlation is used to determine the MRI parameters for each voxel. After analyzing all the voxels, parametric maps are generated. The promising potential of MRF lies in its ability to accurately detect and identify specific structural characteristics, enabling the diagnosis of a

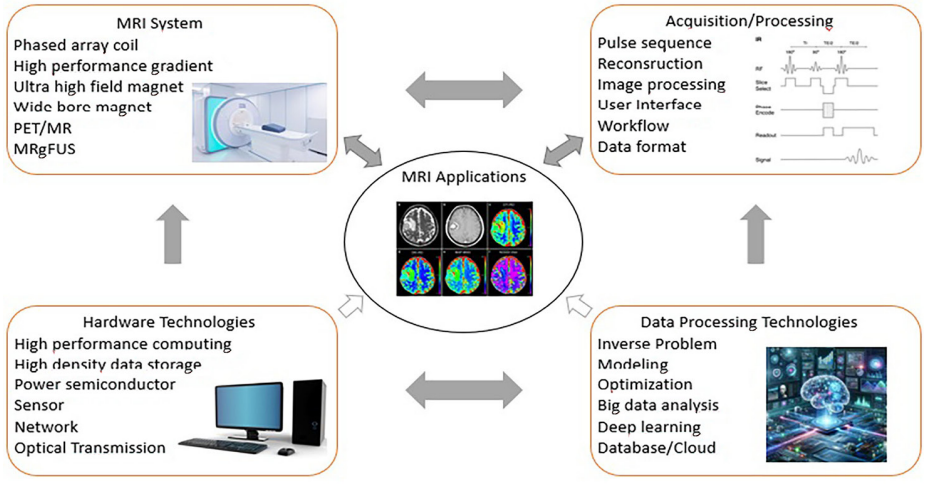

Figure 2. The advancements in MRI technology and the interconnections among its technical components. Advancements in fundamental sciences and engineering have a significant influence on MRI technology. Innovations in each component stimulate advancements in others. MRI, magnetic resonance imaging; MRgFUS, MR-guided focused ultrasound; PET, positron emission tomography.

wide range of clinical diseases. Novel methodologies, such as quantitative sequencing, enable the rapid and precise mapping of dynamic physiological processes. These approaches can evaluate blood flow in cardiac assessments by calculating scalar or vector velocities. A study was conducted to determine scalar velocities perpendicular to a vascular slice using multiparametric T1, T2, and proton density (PD) data. However, these methods are limited by their reliance on physical models to simulate the physiological events being mapped, which may result in potential data loss. Moreover, the complex nature of these models often requires considerable computational resources, thereby prolonging the time required for data collection.[39]

2c. Functional application through magnetic resonance imaging

Blood oxygenation-level dependent (BOLD) imaging, sometimes referred to as functional MRI (fMRI), was developed to indirectly assess neural activity in the brain by examining changes in blood oxygenation associated with brain activity. This type of imaging utilizes the neurovascular response of hyperemia, in which specific brain activity leads to increased blood oxygenation in the stimulated area (Figure 3). Conventional procedures for BOLD imaging typically employ T2 weighting and scan durations of less than 5 seconds to record the hemodynamic response function. Since its inception, the use of BOLD imaging has expanded significantly.[46]

The dependence of the BOLD signal on neurovascular mechanisms introduces specific constraints on fMRI, primarily because the hemodynamic response is slower than the underlying brain activity. This disparity means that the precise timing of neuronal spiking events is largely obscured. To isolate the signal activity associated with these events, mathematical processing techniques such as the general linear model or experimental block protocols are used. By employing these techniques, a temporal resolution of 100 milliseconds can be achieved, which is roughly one-tenth the speed of the brain activities being observed.[39]

An additional challenge encountered by fMRI is the constrained SNR, resulting from limitations in data acquisition and preprocessing. Researchers are actively exploring the use of strong magnetic fields to enhance the accuracy of anatomical imaging to address this challenge. Although most fMRI scans are conducted using three T fields, there is a growing trend toward employing seven T fields. Higher field strengths can reduce the need for spatial smoothing and improve the correlation coefficients of neuronal activity in resting-state networks (RSNs), indicating enhanced spatial resolution.[47]

An effective approach to overcome the time constraints of fMRI is to employ multimodal methods, which combine fMRI with techniques such as EEG or MEG. Both EEG and MEG provide quick temporal responses, capable of identifying brain events with millisecond precision. The reason for integrating these techniques with fMRI is their notably improved temporal resolution. Recent technical improvements enable the concurrent recording of EEG and fMRI signals, enhancing our comprehension of the spatial and temporal characteristics of physiological signals. Nevertheless, compared with fMRI alone, these integrated methodologies are less commonly employed. EEG has a poorer spatial resolution than fMRI, whereas MEG encounters difficulties in accurately determining the source of activity. Hence, to draw any experimental or clinical conclusions, it is imperative for experimental designs or clinical assessments utilizing these integrated methodologies to precisely ascertain the source of the signals.[48]

The persistent difficulties in understanding multimodal approaches have stimulated a longstanding desire to create alternative techniques that provide both precise spatial and temporal resolution. A novel method has been devised that combines the identification of extremely low magnetic fields generated by cerebral electrical activity with the detection of the hemodynamic response using fMRI. The technique, referred to as direct imaging of neuronal activity for fMRI, employs alternating K-space lines to capture the hemodynamic response while directly measuring the ultra-weak magnetic field using another K-space line. Thus far, this methodology has exclusively been utilized in animal models.[49]

A significant advancement in fMRI is the development of resting-state fMRI (RS-fMRI), which examines the inherent, involuntary oscillations in the BOLD signal with a frequency below 0.1 Hz without requiring any specific activities. The functional importance of these variances was first identified in 1995 a study where participants were instructed to abstain from engaging in any cognitive, verbal, or motor tasks. By analyzing the correlation between the BOLD signal time course in a particular brain region that is stimulated by bilateral finger tapping and the signals in other brain areas, the researchers discovered a strong association between changes in activity in the left somatosensory cortex and changes in activity in the corresponding region of the opposite hemisphere. This finding led to the deduction that these "resting networks" reflect the brain's functional connections. Following that, the analysis of spontaneous, synchronized fluctuations in activity across different regions of the brain has resulted in studies that have discovered a spectrum of 7–17 enduring networks, with 7 consistently recognized.[39,50]

RSNs in the human brain are mostly identified through the analysis of BOLD signals. This analysis is based on fMRI's capacity to detect neuronal activity. RS-fMRI relies on

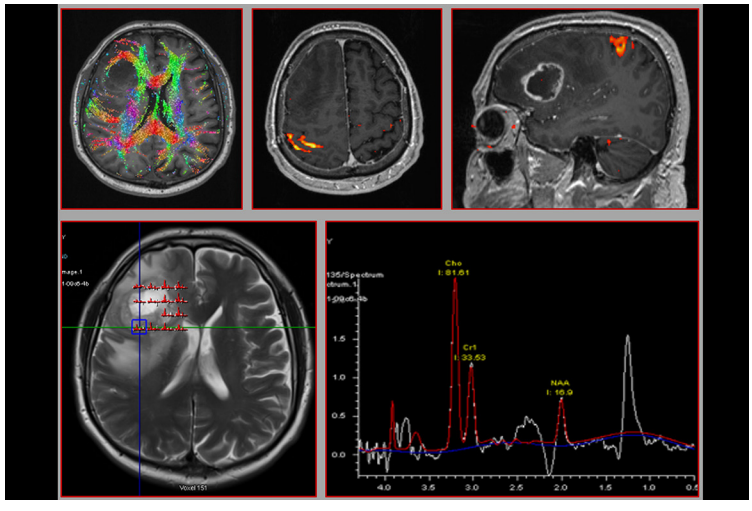

Figure 3. Multiparametric MR images (DTI, MRS, and BOLD fMRI) demonstrate functional activity in the right motor cortex. The images also evaluate the relationship between mass and the motor cortex. MR, magnetic resonance; DTI, diffusion tensor imaging; MRS, magnetic resonance spectroscopy; BOLD fMRI, blood oxygenation-level dependent functional magnetic resonance imaging.

the BOLD signal, which allows for the indirect monitoring of brain activity. This technique shares the advantages of fMRI, such as the ability to observe neural activity, but it has its intrinsic limitations. The primary constraint of fMRI is its temporal resolution, which is limited by the time it takes for the hemodynamic response. Therefore, one essential component of RS-fMRI use is the quantification of fluctuations in brain activity rather than directly recording instances of spiking.[39]

In the initial investigations of RSN functional connectivity, researchers chose specific areas of interest (ROIs) according to their own preferences chose specific regions of interest according to their preferences. Although the ROI technique is simple and easily understandable, its efficiency in discovering new networks is limited due to its dependence on user-defined regions. This is because it is restricted by specified criteria. As a result of this constraint, as well as progress in mathematical modeling and processing capacity, there has been a transition from imposing initial conditions on data to extracting patterns of brain activity directly from the unprocessed time series. An exemplary illustration of this novel methodology is independent component analysis (ICA), which posits that the time series signal arises from numerous spatiotemporal processes that are statistically independent of each other. Through the process of separating these autonomous signals, scientists are able to create chronological sequences for particular parts of the brain and organize them into maps that depict their spatial arrangement. RS-fMRI data can also be interpreted using graph theory, in which nodes represent activity sources and edges characterize the connectivity between these nodes. Unlike ICA, which primarily emphasizes the strength of correlations between distinct areas, graph theory specifically investigates the characteristics of network structure. The interconnections between nodes are characterized by graph metrics, including average path length, clustering coefficients, node degree, centrality measurements, and modularity levels. Graph theory is a potentially valuable tool for investigating how networks in the brain combine and separate. Modularity, a measure of the presence of functionally distinct components or modules within RSNs, is a key tool for characterizing functional changes in behavior, network disturbances, or diseases. This method has uncovered substantial modifications in situations such as stroke and psychiatric disorders.[39,51,52]

Theoretically, conclusions concerning causation based on directed functional connectivity can be expanded to include overall neural activity across the brain. Empirical investigations utilizing RS-fMRI have demonstrated that RSNs can be differentiated based on their metastability and synchronization. These observations have resulted in theories of brain function and behavior that propose that the human brain operates at maximal metastability when at rest, indicating an ideal state of network switching. Identifying the characteristics of RSNs, such as metastability, suggests that changes in directed connectivity could be used to evaluate the development of various brain states. This presents the methodological challenge of creating a descriptive methodology that links functional neuroimaging data to the overall dynamics of the entire brain. Recent efforts to address this challenge have pursued two primary methodologies.[53,54]

2d. Arthrographic applications in magnetic resonance imaging

Joint bone structures can be evaluated successfully using conventional radiographs and CT scans. However, these modalities do not enable the examination of soft tissue stabilizers. MRI, MR arthrography, and CT arthrography are the preferred imaging techniques for evaluating the labral, meniscal, fibrocartilaginous, capsular, and ligamentous structures of joints (Figures 4-6). Routine joint MR examination pulse sequences include fast spin-echo PD with fat suppression, T1- and T2-weighted fast spin-echo without fat saturation, and, occasionally, short tau inversion recovery (STIR). Conventional MRI sequences allow the non-invasive evaluation of tendon pathologies. However, labroligamentous and chondral lesions in these sequences are frequently overlooked. Direct MR arthrography with the intra-articular injection of diluted contrast media is a more sensitive imaging modality for evaluating stabilizers, such as the labrum, joint capsule, and ligaments.[55-60] In an imaging study that used arthroscopy as a reference standard, Gusmer et al.[61] found that conventional MRI has 86% sensitivity for detecting superior labral tears and 74% sensitivity for detecting posterior labral tears (Figure 7). However, despite improvements in image quality, routine MRIs may underestimate the exact extent of tears of the glenoid labrum.[60-62] Moreover, labrocapsular variant anomalies can be misdiagnosed as labral pathologies.[56,63]

Because of increased intra-articular fluid in patients with acute joint injuries, fluid-sensitive MR sequences such as PD, STIR, and T2-weighted imaging can reveal intra-articular damage, including labroligamentous, cartilaginous, and capsular injuries. However, in patients with chronic repetitive trauma, direct MR arthrography demonstrates clear diagnostic superiority over conventional MRI. Direct MR arthrography involves the intra-articular injection of diluted contrast media (gadolinium chelate). This technique allows for the optimal and separate evaluation of intra-articular structures with adequate capsular distension. Moreover, capsular distension in direct MR arthrography permits the leakage of contrast material into the labral substance or sublabral location in cases of labral tears or detachments (Figures 8 and 9). This makes it easier to identify pathologies of the glenoid or acetabular labrum.

Fluoroscopy-guided intra-articular injections for arthrography have been commonly employed since 1975.[64] However, many authors now advocate for performing injection procedures under ultrasonography guidance to avoid damaging anatomical structures along the injection pathway.[65-68] Real-time ultrasonographic guidance for arthrographic examination eliminates exposure to iodinated contrast material and ionizing radiation. In our routine practice, we use sonographic guidance for various approaches: the posterior approach for shoulder arthrography, the

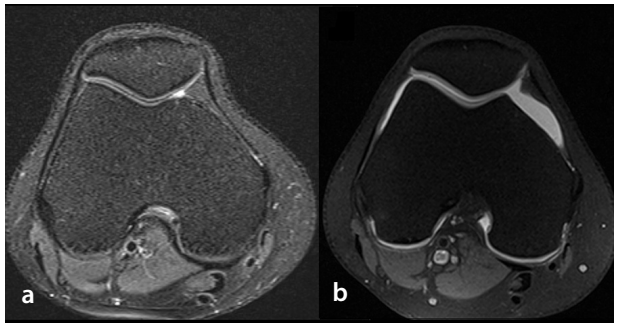

Figure 4. (b) Axial T1-weighted knee MR arthrogram obtained following intra-articular gadolinium injection shows the articular cartilage and capsule more clearly than pre-arthrographic axial PD MR imaging (**a**). MR, magnetic resonance; PD, proton density.

anteromedial approach for ankle arthrography, the anterolateral approach for hip arthrography, the dorsal–radial approach for wrist arthrography, the lateral approach for elbow arthrography, and the anterolateral approach for knee arthrography.

In arthrographic procedures, a sufficient volume of contrast solution is injected until the joint capsule is adequately dilated. The solution volume is determined based on the resistance encountered during injection and the patient's comfort level. The diluted gadolinium solution used for all joint arthrography procedures should have a concentration of 1:200. Table 1 shows the arthrographic solution volume and needle size for each joint.

A thin-section three-dimensional (3D) MR arthrography sequence, such as the fat-suppressed T1-weighted volumetric interpolated breath-hold examination (VIBE), allows for multiplanar reconstruction using submillimetric image slices. 3D VIBE MR arthrography not only provides excellent contrast for labroligamentous structures but also allows the optimal evaluation of the fibrocartilaginous complex and subchondral bone structure (Figure 10). In recent years, the 3D high-resolution T1-weighted VIBE MR arthrography sequence has been successfully employed for diagnosing glenoid bare spot, illustrating intra-articular small ligamentous structures, describing the aponeurotic expansion of the supraspinatus tendon, demonstrating glenoid cartilage defects accompanied by labral pathologies, and evaluating glenohumeral joint capacity for diagnosing primary adhesive capsulitis.[22-24,69-72] Lastly, MR arthrographic examinations with stress maneuvers have been successfully used to investigate capsular abnormalities of the shoulder joint.[73]

2e. Magnetic resonance spectroscopy and cerebrospinal fluid flowmetry

When placed in a strong magnetic field, hydrogen nuclei (protons) exhibit magnetic properties, serving as the source of measurable signals in MRI. The protons in water molecules are the primary source of the signal in MR examinations. However, protons in different molecules display slight magnetic variations, and this subtle difference enables the identification of small molecules in MR spectroscopy (MRS).[74] If the molecules are mobile and present in measurable quantities, MRS can depict these molecules within tissues on the MR spectrum (Figure 11).[75] The raw signal obtained by MRS is dominated by water,

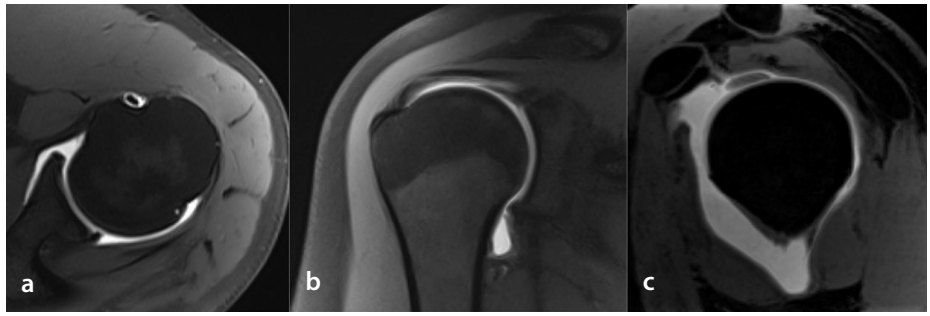

Figure 5. Axial **(a)**, coronal oblique **(b)**, and sagittal oblique **(c)** shoulder MR arthrograms optimally demonstrate the joint capsule, labroligamentous structures, and the underside of the rotator cuff tendons. MR, magnetic resonance.

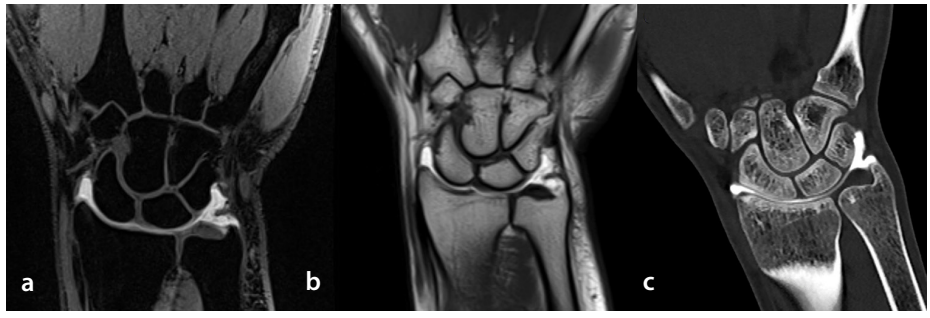

Figure 6. Coronal plane T1-weighted VIBE, TSE T1, and multi-detector CT arthrograms of the radiocarpal joint clearly reveal the cartilaginous surface, joint capsule, and triangular fibrocartilaginous complex. VIBE, volumetric interpolated breath-hold examination; CT, computed tomography.

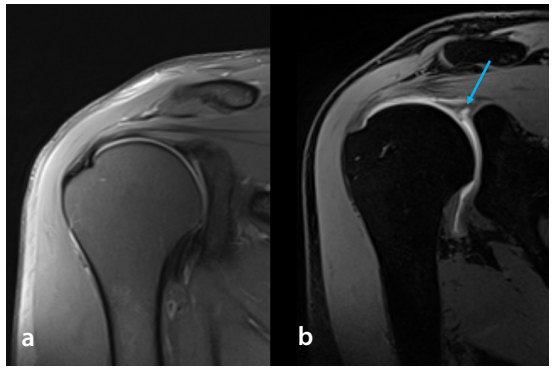

Figure 7. Coronal oblique plane PD MR imaging **(a)** of the right glenohumeral joint shows no pathology in the superior labrum; however, T1-weighted VIBE MR arthrography **(b)** reveals a type 2 SLAP lesion (blue arrow). PD, proton density; MR, magnetic resonance; VIBE, volumetric interpolated breath-hold examination.

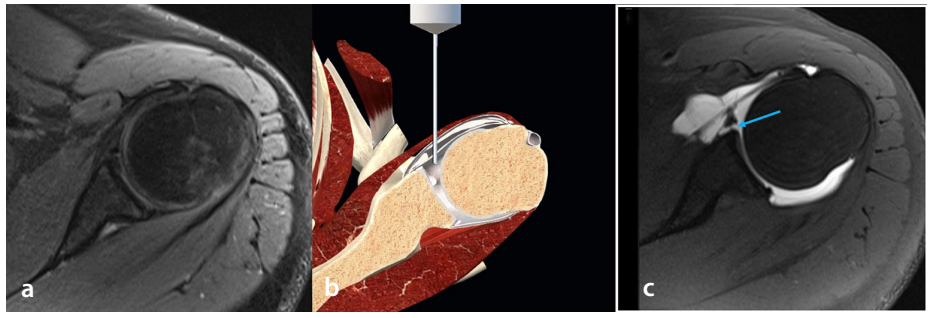

Figure 8. Transverse PD MR imaging **(a)** of the left glenohumeral joint shows no pathology in the anterior labrum; however, after Gd injection into the articular space **(b)**, SE T1-weighted MR arthrography **(c)** clearly reveals a fibrous Bankart lesion (blue arrow). [The illustration was created using Adobe Photoshop (Adobe Inc., 2021 Adobe Photoshop, https://www.adobe.com/products/photoshop.html) based on figures provided by the Complete Anatomy program (3D4 Medical, 2021. Complete Anatomy. Retrieved from https://3d4medical.com/)]. PD, proton density; MR, magnetic resonance; Gd, gadolinium; SE, spin-echo.

rendering signals from other metabolites invisible. To address this issue, water suppression techniques are employed, allowing for a clear and useful spectrum. MRS is not only used for differential diagnosis in neuroradiology, particularly in brain tissue, but also in other parts of the body,[76-78] focusing on specific metabolites of the targeted tissue.

Another advanced MRI technique, cerebrospinal fluid (CSF) flowmetry, is used to assess CSF through both qualitative and quantitative approaches (Figure 12). Time-resolved 2D phase-contrast MRI with velocity encoding is the most commonly employed method for this examination. The measured flow parameters in this technique reflect the pulsatile (to-and-fro) movement of CSF caused by vascular pulsations rather than the slow CSF transfer along the glymphatic pathway. This technique relies on the sequential, location-specific application of a pair of phase-encoding pulses in opposite directions. Stationary protons, which experience the same pulse in both instances, produce no signal. By contrast, moving protons, which encounter altered phase-encoding pulses, are rendered visible.[79] CSF flowmetry studies are particularly useful in evaluating clinical conditions such as normal pressure hydrocephalus, the patency of third ventriculostomy, aqueductal stenosis, and CSF flow at the cervicomedullary junction.[80]

2f. Artificial intelligence

AI has revolutionized MRI by introducing a wide range of applications that improve image acquisition, analysis, and therapeutic decision-making. The integration of AI into MRI has ushered in a new era in medical imaging, offering substantial benefits to both patients and healthcare providers. Table 2 summarizes how AI enhances various aspects of MRI, including improving image quality, facilitating disease diagnosis, and supporting treatment planning.[81]

3. Ultrasound

Ultrasound (US) is a versatile imaging technique widely used as an initial diagnostic method in various clinical scenarios worldwide. Continuous advancements in US technology provide new opportunities for medical diagnoses and therapies, solidifying its importance in medical imaging.

A 3D imaging method has been developed to overcome the limitations of traditional 2D US. This innovation allows the visualization of 3D anatomy, precise transducer adjustments for optimal disease monitoring, and accurate volume measurements. Several techniques have been developed for producing 3D US images; these include mechanical and free-hand scanning with linear arrays and the use of 2D arrays for real-time 3D imaging, also known as 4D US. Mechanical scanning utilizes a motorized mechanism to move a standard transducer and algorithms to construct 3D images from 2D scans. A motor/encoder ensures accurate information on the positions and orientations of the 2D US images, enabling the precise adjustment of the scanning geometry.[82]

Calibration is a crucial step in 3D reconstruction. It involves determining the position and angle of the position sensor relative to the US image. Various methods can achieve this. One successful approach enhances the spatial calibration of probes in 3D free-hand ultrasonic scanning. This method

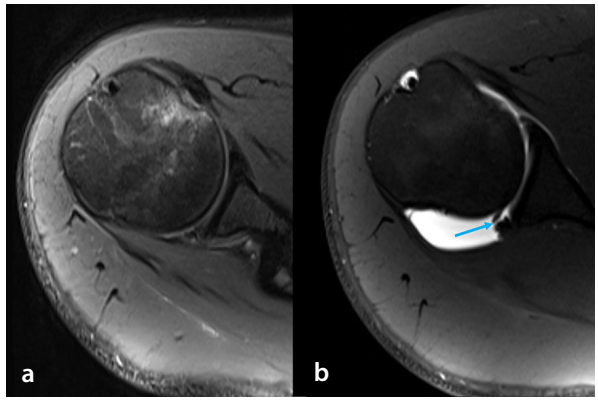

Figure 9. Transverse plane PD MR imaging **(a)** of the right glenohumeral joint shows no pathological findings in the posterior labrum; however, SE T1-weighted MR arthrography **(b)** clearly reveals a posterior labral defect (blue arrow). PD, proton density; MR, magnetic resonance; SE, spin-echo.

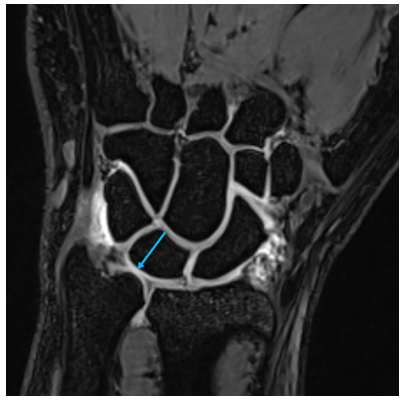

Figure 10. Coronal plane T1-weighted VIBE MR arthrography of the radiocarpal joint shows a central rupture (blue arrow) of the triangular fibrocartilaginous complex. VIBE, volumetric interpolated breath-hold examination; MR, magnetic resonance.

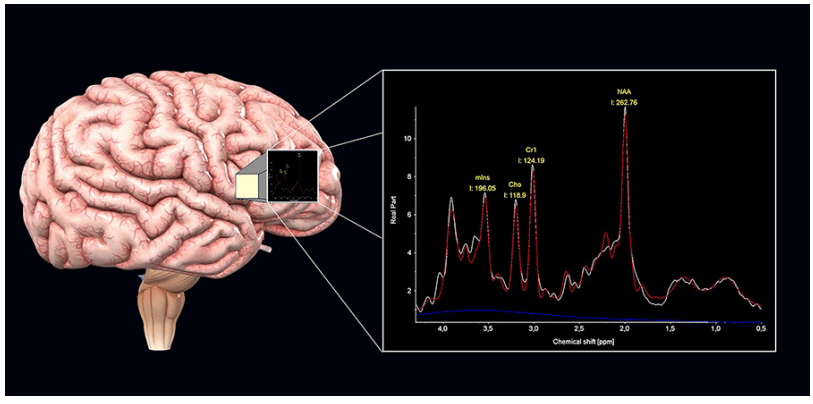

Figure 11. Measuring metabolites of the brain using MR spectroscopy [the illustration was created using Adobe Photoshop (Adobe Inc., 2021 Adobe Photoshop, https://www.adobe.com/products/photoshop.html) based on figures provided by the Complete Anatomy program (3D4 Medical, 2021. Complete Anatomy. Retrieved from https://3d4medical.com/)]. MR, magnetic resonance.

identifies similarity measures between two image sets-one from a 2D sweep and the other from a 3D reconstruction taken in a perpendicular sweep. However, a limitation of mechanical or free-hand scanning is the relatively slow volume capture rate, typically 2–3 volumes per second, which can hinder 3D imaging efficiency.[83]

The implementation of transducers equipped with 2D phased arrays for real-time 3D imaging has greatly enhanced the rate at which volume acquisition occurs. These transducers use electronic scanning to collect 3D data by producing a diverging beam in a pyramidal shape. The received echoes are then processed to create real-time 3D images. To further enhance high-volume imaging rates, a wideband 2D sparse array paired with multiline receiving has been proposed. This approach optimizes the use of a limited number of active components while maintaining a high level of accuracy and speed.[82,83]

A critical aspect of 3D imaging is the representation of the generated images, commonly achieved through multiplanar reformatting or volume rendering. However, the spatial resolution of 3D imaging is anisotropic and is typically inferior to that of 2D imaging. This limitation arises because the spacing between the collected 2D images increases with depth, resulting in reduced resolution at greater depths.[83]

Elastography is an advanced imaging technique that uses US to assess tissue stiffness, enhancing the diagnostic capabilities of B-mode US. Two primary methods of elastography are employed in evaluating breast lesions, shear wave elastography (SWE) and strain elastography. Although strain elastography requires operator expertise, SWE relies on focused radiation forces and eliminates the need for manual compression, making it operator independent.[84]

SWE is widely used in diagnosing tumoral and inflammatory pathologies in many organs, with research in these areas steadily growing. Moreover, recent studies suggest that SWE may also play a role in monitoring treatment efficacy.[84-86]

AI technology has the potential to create more accurate and repeatable outcomes in US examinations. AI and computer-assisted technologies can standardize medical processes, reduce training and examination durations, and improve the quality of US images across four main study areas. Leveraging machine learning in US imaging holds considerable promise for enhancing image quality, providing clearer and more practical visuals, and introducing novel US imaging techniques. Advancements in beamforming, super-resolution, and image enhancement often require hardware modifications, which are typically more complex than straightforward software upgrades. Despite these challenges, many recent research advancements outperform conventional reconstruction algorithms, which transform ultrasonic wave measurements into display visuals. The enhanced processing capabilities of medical devices now support the integration of increasingly sophisticated real-time solutions in a range of US imaging approaches. AI algorithms can aid healthcare professionals-including physicians, nurses, and technicians-in performing comprehensive US scans, thereby simplifying the learning pro-

Table 2. Concise overview of how AI improves several elements of MRI

Submission	Description
Image enhancement	Reduces noise and artifacts in MRI images. Enhances image resolution for finer anatomical details
Image reconstruction	Enables faster MRI scans. Reconstructs high-quality images from sparsely sampled data
Disease detection and diagnosis	Identifies and characterizes tumors in MRI scans. Aids in diagnosing conditions such as Alzheimer's using brain MRI. Assists in detecting heart diseases via cardiac MRI
Lesion segmentation	Accurately segments lesions in MRI scans, aiding in treatment planning
Functional MRI analysis	Maps brain regions activated during tasks or conditions, facilitating cognitive research
Diffusion MRI analysis	Reconstructs white matter tracts in the brain, which are valuable for neurosurgical planning
Quantitative imaging	Quantifies tissue properties (T1, T2, diffusion) for disease characterization. AI analyzes tissue perfusion in MRI, which is important for diagnosing conditions such as stroke
Automated reporting	Generates automated radiology reports by extracting findings from MRI scans
Treatment planning	Assists in radiotherapy planning by delineating target volumes on MRI
Monitoring disease progression	Tracks disease progression by analyzing changes in MRI scans over time
Predictive modeling	Predicts disease outcomes and treatment responses based on MRI data
Quality control	Performs quality checks on MRI scans, flagging artifacts and anomalies
Population studies	Analyzes large MRI datasets for trends, risk factors, and early disease indicators
Customization and personalization	Tailors MRI protocols to individual patients for optimized imaging

AI, artificial intelligence; MRI, magnetic resonance imaging.

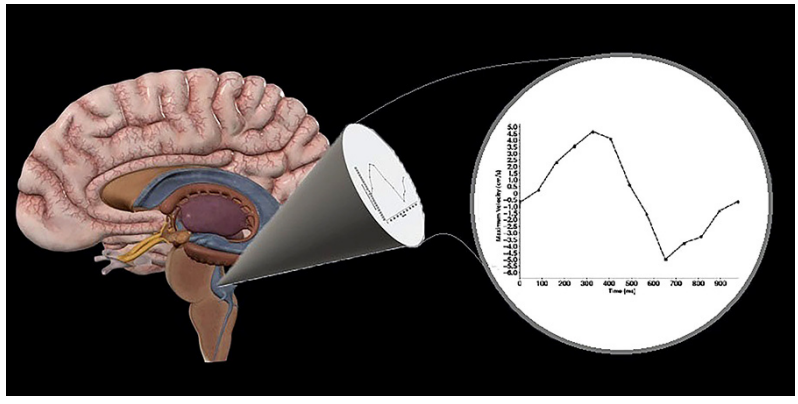

Figure 12. CSF flow analysis using CSF flowmetry [the illustration was created using Adobe Photoshop (Adobe Inc., 2021 Adobe Photoshop, https://www.adobe.com/products/photoshop.html) based on figures provided by the Complete Anatomy program (3D4 Medical, 2021. Complete Anatomy. Retrieved from https://3d4medical.com/)]. CSF, cerebrospinal fluid.

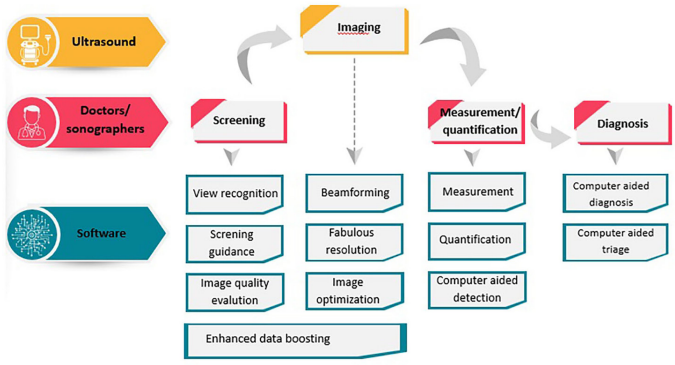

Figure 13. Effects of technological advancements on ultrasonographic imaging steps.

cess. Modern image processing algorithms used for measurement, quantification, and computer-aided detection have evolved beyond conventional feature engineering. The latest US imaging systems utilize advanced deep learning approaches. Computer-assisted diagnosis, triage, detection, and quantification are currently receiving considerable academic attention for their potential to reduce the workload of physicians (Figure 13).[87]

In conclusion, the field of radiography is being significantly influenced by technological advancements, potentially more so than other areas of medicine. Current developments in CT technology primarily focus on reducing the dosage of the ionizing radiation administered to patients. By contrast, progress in MRI systems is centered around improving accessibility, shortening scan durations, and generating high-quality images in regions where MRI has traditionally faced challenges. Furthermore, the development of portable devices for bedside use is becoming an increasingly important objective in both CT and MRI. Sonography innovations are advancing to enhance image quality and expand the applications of elastography. AI technology holds great potential for producing more accurate and repeatable results in US exams, enhancing image quality, generating clearer and more useful images, and even developing new US imaging techniques. Furthermore, AI technologies are being increasingly integrated into CT and MRI, with a growing focus on improving image production, enhancing image quality, and facilitating image evaluation.

Footnotes

Conflict of interest disclosure

Sonay Aydın, MD, is Section Editor in Diagnostic and Interventional Radiology. He had no involvement in the peer-review of this article and had no access to information regarding its peer-review. Other authors have nothing to disclose.

References

1. Hussain S, Mubeen I, Ullah N, et al. Modern diagnostic imaging technique applications and risk factors in the medical field: a review. *Biomed Res Int*. 2022;2022:5164970. [CrossRef]
2. Kasban H, El-Bendary M, Salama D. A comparative study of medical imaging techniques. *International Journal of Information Science and Intelligent System*. 2015;4(2):37-58. [CrossRef]
3. Roobottom CA, Mitchell G, Morgan-Hughes G. Radiation-reduction strategies in cardiac computed tomographic angiography. *Clin Radiol*. 2010;65(11):859-867. [CrossRef]
4. McPhee SJ, Papadakis MA, Rabow MW. Current medical diagnosis & treatment 2010: McGraw-Hill Medical New York: 2010. [CrossRef]
5. Mooney LR. A middle English verse compendium of astrological medicine. Med Hist. 1984;28(4):406-419. [CrossRef]
6. Berger D. A brief history of medical diagnosis and the birth of the clinical laboratory. Part 1--Ancient times through the 19th century. MLO Med Lab Obs. 1999;31(7):28-40. [CrossRef]
7. Bradley WG. History of medical imaging. *Proc Am Philos Soc*. 2008;152(3):349-361. [CrossRef]
8. Schulz RA, Stein JA, Pelc NJ. How CT happened: the early development of medical computed tomography. J Med Imaging. 2021;8(5):052110. [CrossRef]
9. Stański M, Michałowska I, Lemanowicz A, et al. Dual-energy and photon-counting computed tomography in vascular applications-technical background and post-processing techniques. *Diagnostics (Basel)*. 2024;14(12):1223. [CrossRef]
10. McCollough CH, Leng S, Yu L, Fletcher JG. Dual- and Multi-Energy CT: principles, technical approaches, and clinical applications. *Radiology*. 2015;276(3):637-653. [CrossRef]
11. Parakh A, Lennartz S, An C, et al. Dual-energy CT images: pearls and pitfalls. *Radiographics*. 2021;41(1):98-119. [CrossRef]
12. Toshav A. Economics of dual-energy CT: workflow, costs, and benefits. *Semin Ultrasound CT MR*. 2022;43(4):352-354. [CrossRef]
13. Wong WD, Mohammed MF, Nicolaou S, et al. Impact of dual-energy CT in the emergency department: increased radiologist confidence, reduced need for follow-up imaging, and projected cost benefit. *AJR Am J Roentgenol*. 2020;215(6):1528-1538. [CrossRef]
14. Burch RA, Siddiqui TA, Tou LC, Turner KB, Umair M. The cost effectiveness of coronary CT angiography and the effective utilization of CT-fractional flow reserve in the diagnosis of coronary artery disease. *J Cardiovasc Dev Dis*. 2023;10(1):25. [CrossRef]
15. Aydın S, Karavaş E, Ünver E, Şenbil DC, Kantarcı M. Long-term lung perfusion changes related to COVID-19: a dual energy computed tomography study. *Diagn Interv Radiol*. 2023;29(1):103-108. [CrossRef]
16. Aydin S, Kantarci M, Karavas E, Unver E, Yalcin S, Aydin F. Lung perfusion changes in COVID-19 pneumonia: a dual energy computerized tomography study. *Br J Radiol*. 2021;94(1125):20201380. [CrossRef]
17. Kantarcı M, Bayraktutan Ü, Akbulut A, et al. The value of dual-energy computed tomography in the evaluation of myocarditis. *Diagn Interv Radiol*. 2023;29(2):276-282. [CrossRef]
18. Cetin T, Kantarci M, Irgul B, et al. Quadruple-rule-out computed tomography angiography (QRO-CT): a novel dual-energy computed tomography technique for the diagnostic work-up of acute chest pain. *Diagnostics (Basel)*. 2023;13(17):2799. [CrossRef]
19. Rajendran K, Petersilka M, Henning A, et al. Full field-of-view, high-resolution, photon-counting detector CT: technical assessment and initial patient experience. *Phys Med Biol*. 2021;66(20):10. [CrossRef]
20. Rajendran K, Petersilka M, Henning A, et al. First clinical photon-counting detector CT system: technical evaluation. *Radiology*. 2022;303(1):130-138. [CrossRef]
21. Zhao C, Martin T, Shao X, Alger JR, Duddalwar V, Wang DJJ. Low dose CT perfusion with K-space weighted image average (KWIA). *IEEE Trans Med Imaging*. 2020;39(12):3879-3890. [CrossRef]
22. Gokce A, Guclu D, Unlu EN, Kazoglu I, Arican M, Ogul H. Comparison of conventional MR arthrography and 3D volumetric MR arthrography in detection of cartilage defects accompanying glenoid labrum pathologies. *Skeletal Radiol*. 2024;53(6):1081-1090. [CrossRef]
23. Ozel MA, Ogul H, Koksal A, et al. Detection of the glenoid bare spot by non-arthrographic MR imaging, conventional MR arthrography,

and 3D high-resolution T1-weighted VIBE MR arthrography: comparison with CT arthrography. *Eur Radiol*. 2023;33(5):3276-3285. [CrossRef]

24. Ogul H, Taydas O, Sakci Z, Altinsoy HB, Kantarci M. Posterior shoulder labrocapsular structures in all aspects; 3D volumetric MR arthrography study. *Br J Radiol*. 2021;94(1123):20201230. [CrossRef]
25. Polat G, Oğul H, Yalçin A, et al. Efficacy of the rotational traction method in the assessment of glenohumeral cartilage surface area in computed tomography arthrography. *J Comput Assist Tomogr*. 2019;43(2):345-349. [CrossRef]
26. Ogul H, Taydas O, Tuncer K, Polat G, Pirimoglu B, Kantarci M. MR arthrographic evaluation of the association between anterolateral soft tissue impingement and osteochondral lesion of the tibiotalar joint. *Radiol Med*. 2019;124(7):653-661. [CrossRef]
27. Ogul H, Cankaya B, Kantarci M. The distribution in joint recesses and adjacent synovial compartments of loose bodies determined on MR and CT arthrographies of ankle joint. *Br J Radiol*. 2022;95(1132):20201239. [CrossRef]
28. Zagarella A, Signorelli G, Muscogiuri G, et al. Overuse-related instability of the elbow: the role of CT-arthrography. *Insights Imaging*. 2022;12(1):140. [CrossRef]
29. Demehri S, Muhit A, Zbijewski W, et al. Assessment of image quality in soft tissue and bone visualization tasks for a dedicated extremity cone-beam CT system. *Eur Radiol*. 2015;25(6):1742-1751. [CrossRef]
30. Posadzy M, Desimpel J, Vanhoenacker F. Cone beam CT of the musculoskeletal system: clinical applications. *Insights Imaging*. 2018;9(1):35-45. [CrossRef]
31. Koskinen SK, Haapamäki VV, Salo J, et al. CT arthrography of the wrist using a novel, mobile, dedicated extremity cone-beam CT (CBCT). *Skeletal Radiol*. 2013;42(5):649-657. [CrossRef]
32. Koivisto J, Kiljunen T, Kadesjö N, Shi XQ, Wolff J. Effective radiation dose of a MSCT, two CBCT and one conventional radiography device in the ankle region. *J Foot Ankle Res*. 2015;8:8. [CrossRef]
33. Haridas H, Mohan A, Papisetti S, Ealla KK. Computed tomography: will the slices reveal the truth. *J Int Soc Prev Community Dent*. 2016;6(Suppl 2):85-92. [CrossRef]
34. Karaca L, Yuceler Z, Kantarci M, et al. The feasibility of dual-energy CT in differentiation of vertebral compression fractures. *Br J Radiol*. 2016;89(1057):20150300. [CrossRef]
35. Park EH, O'Donnell T, Fritz J. Dual-energy computed tomography applications in rheumatology. *Radiol Clin North Am*. 2024;62(5):849-863. [CrossRef]
36. Sandhu R, Aslan M, Obuchowski N, Primak A, Karim W, Subhas N. Dual-energy CT arthrography: a feasibility study. *Skeletal Radiol*. 2021;50(4):693-703. [CrossRef]
37. Foti G, Booz C, Buculo GM, et al. Dual-energy CT arthrography: advanced muscolo-skelatal applications in clinical practice. *Tomography*. 2023;9(4):1471-1484. [CrossRef]
38. Stern C, Graf DN, Bouaicha S, Wieser K, Rosskopf AB, Sutter R. Virtual non-contrast images calculated from dual-energy CT shoulder arthrography improve the detection of intraarticular loose bodies. *Skeletal Radiol*. 2022;51(8):1639-1647. [CrossRef]
39. Larrivee D. Introductory chapter: new advances in MRI clinical analysis. *New Advances in Magnetic Resonance Imaging: IntechOpen*. 2024. [CrossRef]
40. Gordon Y, Partovi S, Müller-Eschner M, et al. Dynamic contrast-enhanced magnetic resonance imaging: fundamentals and application to the evaluation of the peripheral perfusion. *Cardiovasc Diagn Ther*. 2014;4(2):147-164. [CrossRef]
41. Vadmal V, Junno G, Badve C, Huang W, Waite KA, Barnholtz-Sloan JS. MRI image analysis methods and applications: an algorithmic perspective using brain tumors as an exemplar. *Neurooncol Adv*. 2020;2(1):vdaa049. [CrossRef]
42. Khalil M, Ayad H, Adib A. Performance evaluation of feature extraction techniques in MR-brain image classification system. *Procedia Comput Sci*. 2018;127:218-225. [CrossRef]
43. Ma D, Gulani V, Seiberlich N, et al. Magnetic resonance fingerprinting. *Nature*. 2013;495(7440):187-192. [CrossRef]
44. Fayaz M, Torokeldiev N, Turdumamatov S, et al. An efficient methodology for brain MRI classification based on DWT and convolutional neural network. *Sensors (Basel)*. 2021;21(22):7480. [CrossRef]
45. Yacoub E, Van De Moortele PF, Shmuel A, Uğurbil K. Signal and noise characteristics of Hahn SE and GE BOLD fMRI at 7 T in humans. *Neuroimage*. 2005;24(3):738-750. [CrossRef]
46. Loued-Khenissi L, Döll O, Preuschoff K. An overview of functional magnetic resonance imaging techniques for organizational research. *Organ Res Methods*. 2019;22(1):17-45. [CrossRef]
47. Raimondo L, Oliveira ĹAF, Heij J, et al. Advances in resting state fMRI acquisitions for functional connectomics. *Neuroimage*. 2021;243:118503. [CrossRef]
48. Fleury M, Figueiredo P, Vourvopoulos A, Lécuyer A. Two is better? Combining EEG and fMRI for BCI and neurofeedback: a systematic review. *J Neural Eng*. 2023;20(5). [CrossRef]
49. Toi PT, Jang HJ, Min K, et al. In vivo direct imaging of neuronal activity at high temporospatial resolution. *Science*. 2022;378(6616):160-168. [CrossRef]
50. Damoiseaux JS, Rombouts SA, Barkhof F, et al. Consistent resting-state networks across healthy subjects. *Proc Natl Acad Sci U S A*. 2006;103(37):13848-13853. [CrossRef]
51. Corbetta M, Siegel JS, Shulman GL. On the low dimensionality of behavioral deficits and alterations of brain network connectivity after focal injury. *Cortex*. 2018;107:229-237. [CrossRef]
52. Biswal B, Yetkin FZ, Haughton VM, Hyde JS. Functional connectivity in the motor cortex of resting human brain using echo-planar MRI. *Magn Reson Med*. 1995;34(4):537-541. [CrossRef]
53. Beim Graben P, Jimenez-Marin A, Diez I, Cortes JM, Desroches M, Rodrigues S. Metastable resting state brain dynamics. *Front Comput Neurosci*. 2019;13:62. [CrossRef]
54. López-González A, Panda R, Ponce-Alvarez A, et al. Loss of consciousness reduces the stability of brain hubs and the heterogeneity of brain dynamics. *Commun Biol*. 2021;4(1):1037. [CrossRef]
55. Beltran J, Rosenberg ZS, Chandnani VP, Cuomo F, Beltran S, Rokito A. Glenohumeral instability: evaluation with MR arthrography. *Radiographics*. 1997;17(3):657-673. [CrossRef]
56. Ogul H, Tuncer K, Kose M, Pirimoglu B, Kantarci M. MR arthrographic characterization of posterior capsular folds in shoulder joints. *Br J Radiol*. 2019;92(1094):20180527. [CrossRef]
57. Shah N, Tung GA. Imaging signs of posterior glenohumeral instability. *AJR Am J Roentgenol*. 2009;192(3):730-735. [CrossRef]
58. Harish S, Nagar A, Moro J, Pugh D, Rebello R, O'Neill J. Imaging findings in posterior instability of the shoulder. *Skeletal Radiol*. 2008;37(8):693-707. [CrossRef]
59. Chiavaras MM, Harish S, Burr J. MR arthrographic assessment of suspected posteroinferior labral lesions using flexion, adduction, and internal rotation positioning of the arm: preliminary experience. *Skeletal Radiol*. 2010;39(5):481-488. [CrossRef]
60. Ogul H, Ayyildiz V, Pirimoglu B, et al. Magnetic resonance arthrographic demonstration of association of superior labrum anterior and posterior lesions with extended anterior labral tears. *J Comput Assist Tomogr*. 2019;43(1):51-60. [CrossRef]
61. Gusmer PB, Potter HG, Schatz JA, et al. Labral injuries: accuracy of detection with unenhanced MR imaging of the shoulder. *Radiology*. 1996;200(2):519-524. [CrossRef]
62. Lindauer KR, Major NM, Rougier-Chapman DP, Helms CA. MR imaging appearance of 180-360 degrees labral tears of the shoulder. *Skeletal Radiol*. 2005;34(2):74-79. [CrossRef]
63. Ogul H. Evaluation of posterosuperior labral tear with shoulder sonography after intra-articular injection. *Am J Phys Med Rehabil*. 2018;97(11):e110. [CrossRef]

64. Schneider R, Ghelman B, Kaye JJ. A simplified injection technique for shoulder arthrography. *Radiology*. 1975;114(3):738-739. [CrossRef]
65. Ogul H, Bayraktutan U, Yildirim OS, et al. Magnetic resonance arthrography of the glenohumeral joint: ultrasonography-guided technique using a posterior approach. *Eurasian J Med*. 2012;44(2):73-78. [CrossRef]
66. Ogul H, Bayraktutan U, Ozgokce M, et al. Ultrasound-guided shoulder MR arthrography: comparison of rotator interval and posterior approach. *Clin Imaging*. 2014;38(1):11-17. [CrossRef]
67. Zwar RB, Read JW, Noakes JB. Sonographically guided glenohumeral joint injection. *AJR Am J Roentgenol*. 2004;183:48-50. [CrossRef]
68. Souza PM, Aguiar RO, Marchiori E, Bardoe SA. Arthrography of the shoulder: a modified ultrasound guided technique of joint injection at the rotator interval. *Eur J Radiol*. 2010;74(3):29-32. [CrossRef]
69. Ogul H, Tas N, Tuncer K, et al. 3D volumetric MR arthrographic assessment of shoulder joint capacity in patients with primary adhesive capsulitis. *Br J Radiol*. 2019;92(1094):20180496. [CrossRef]
70. Guclu D, Ogul H, Unlu EN, et al. The 2D and 3D MR arthrographic description of aponeurotic expansion of supraspinatus tendon and biceps tendon anomaly in a large patient cohort. *Skeletal Radiol*. 2024;53(2):375. [CrossRef]
71. Ogul H, Karaca L, Can CE, et al. Anatomy, variants, and pathologies of the superior glenohumeral ligament: magnetic resonance imaging with three-dimensional volumetric interpolated breath-hold examination sequence and conventional magnetic resonance arthrography. *Korean J Radiol*. 2014;15(4):508-522. [CrossRef]
72. Cankaya B, Ogul H. An inconspicuous stabilizer of the subtalar joint: MR arthrographic anatomy of the posterior talocalcaneal ligament. *Skeletal Radiol*. 2021;50(4):705-710. [CrossRef]
73. Keles P, Ogul H, Tuncer K, Sakci Z, Ay M, Kantarci M. Magnetic resonance arthrography with positional manoeuvre for the diagnosis of synovial fold of posterior shoulder joint capsule. *Eur Radiol*. 2024. [CrossRef]
74. Sitter B, Sjøbakk TE, Larsson HBW, Kvistad KA. Clinical MR spectroscopy of the brain. *Tidsskr Nor Laegeforen*. 2019;139(6). [CrossRef]
75. Ross B, Bluml S. Magnetic resonance spectroscopy of the human brain. *Anat Rec*. 2001;265(2):54-84. [CrossRef]
76. Engelke K, Chaudry O, Gast L, et al. Magnetic resonance imaging techniques for the quantitative analysis of skeletal muscle: State of the art. *J Orthop Translat*. 2023;42:57-72. [CrossRef]
77. Fardanesh R, Marino MA, Avendano D, Leithner D, Pinker K, Thakur SB. Proton MR spectroscopy in the breast: Technical innovations and clinical applications. *J Magn Reson Imaging*. 2019;50(4):1033-1046. [CrossRef]
78. Verma S, Rajesh A, Fütterer JJ, et al. Prostate MRI and 3D MR spectroscopy: how we do it. *AJR Am J Roentgenol*. 2010;194(6):1414-1426. [CrossRef]
79. Battal B, Kocaoglu M, Bulakbasi N, Husmen G, Tuba Sanal H, Tayfun C. Cerebrospinal fluid flow imaging by using phase-contrast MR technique. *Br J Radiol*. 2011;84(1004):758-765. [CrossRef]
80. Mbonane S, Andronikou S. Interpretation and value of MR CSF flow studies for paediatric neurosurgery. *S Afr J Radiol*. 2013;17(1):26-29. [CrossRef]
81. Turkbey B, Haider MA. Deep learning-based artificial intelligence applications in prostate MRI: brief summary. *Br J Radiol*. 2022;95(1131):20210563. [CrossRef]
82. Golemati S, Cokkinos DD. Recent advances in vascular ultrasound imaging technology and their clinical implications. *Ultrasonics*. 2022;119:106599. [CrossRef]
83. Sciallero C, Trucco A. Wideband 2-D sparse array optimization combined with multiline reception for real-time 3-D medical ultrasound. *Ultrasonics*. 2021;111:106318. [CrossRef]
84. Ece B, Aydin S, Kantarci M. Shear wave elastography-correlated dose modifying: can we reduce corticosteroid doses in idiopathic granulomatous mastitis treatment? Preliminary results. *J Clin Med*. 2023;12(6):2265. [CrossRef]
85. Ece B, Aydin S. Can shear wave elastography help differentiate acute tonsillitis from normal tonsils in pediatric patients: a prospective preliminary study. *Children (Basel)*. 2023;10(4):704. [CrossRef]
86. Cetin T, Tokur O, Bozkurt HB, Aydin S, Memis KB, Kantarci M. Shear wave ultrasonographic elastography in pediatric spleens and its role in differential diagnosis. *Diagnostics (Basel)*. 2024;14(11):1142. [CrossRef]
87. Tenajas R, Miraut D, Illana CI, Alonso-Gonzalez R, Arias-Valcayo F, Herraiz JL. Recent advances in artificial intelligence-assisted ultrasound scanning. *Appl Sci*. 2023;13(6):3693. [CrossRef]